

Cyclotron Resonance and Faraday Effect Measurements using Infrared Spectroscopy

Yinming Shao

*Department of Physics, The University of California at San Diego, La Jolla, California 92093, USA**

In this Letter I will first briefly review the origin, theoretical background and development of cyclotron resonance technique with an emphasis on the free-carrier properties. The theoretical background will be derived using the semi-classical Drude formalism. I will then introduce the magneto-optical Faraday effect and derive the general formula of Faraday rotation angles for a two-dimensional electron gas. I will use graphene as a special case and demonstrate the relationship of conductivity tensor components and the measurable quantities, i.e. absorption and Faraday rotation. The basic technique underlying the measurement of absorption (transmission) and Faraday rotation spectra is Fourier Transform Infrared spectroscopy (FTIR). I will briefly discuss the mechanism of a FTIR and then focus on the recent results of cyclotron resonance and Faraday effect measurement on graphene using this technique.

I. INTRODUCTION

Cyclotron resonance is one of the most direct and accurate tool to measure the effective mass components in semiconductors. The basic idea of cyclotron resonance measurement is that electrons (or holes) undergoes circular motion under the influence of an external DC magnetic field. When an AC electric field is applied perpendicular to the magnetic field, the electrons (or holes) can resonantly absorb energy from the electric field if the field is always in phase with its circular motion. The cyclotron frequency $\omega_c = eB/m$ is found by equating the Lorentz force and the centripetal force and the resonance condition is therefore $\omega = \omega_c$. For free electrons, e is the electron charge, B is the magnetic field and m is the free electron mass. Notice that the cyclotron frequency does not depend on the radius of the orbit so that charge carrier can be excited to larger orbits by absorbing energy from the AC electric field. Under the effective mass approximation, the resonance condition becomes $\omega = \omega_c = eB/m_c$ where m_c denotes the cyclotron mass, defined by:

$$m_c = \frac{\hbar^2}{2\pi} \frac{\partial S}{\partial E} \quad (1)$$

Here S is the cross-sectional area in k space that the cyclotron motion encloses perpendicular to the magnetic field.

For simple parabolic band with dispersion relation:

$$\mathbf{E}(\mathbf{k}) = \frac{\hbar^2 \mathbf{k}^2}{2m^*} \quad (2)$$

Where the effective mass is defined as:

$$(m_{xy}^*)^{-1} = \frac{1}{\hbar^2} \frac{\partial^2 \mathbf{E}(\mathbf{k})}{\partial k_x \partial k_y} \quad (3)$$

The measured cyclotron mass equals the effective mass precisely if the band dispersion is isotropic and parabolic, as can be readily verified. This parabolic (or quadratic)

dependence is valid close to the band extreme (conduction band minimum or valence band maximum) so the effective mass can be approximated by cyclotron mass in many semiconductors where the charge carriers are located mostly near the band extreme.

In practice, both the frequency and the magnetic field can be swept over resonance condition to observe the cyclotron resonance, yielding $m_c = eB/\omega_c$.

Although the idea of cyclotron resonance is simple, one has to satisfy several requirements to successfully observe cyclotron resonance in experiment. First is that the oscillating electric field applied perpendicular to the magnetic field should be able to penetrate the whole sample. In semiconductors this is relatively easy to satisfy at low temperature. However, for metals the charge carrier density becomes so high that E-field can only penetrate a very thin layer called skin depth $\delta = \sqrt{\frac{2}{\sigma \mu \omega}}$. For copper at room temperature, the skin depth is about several μm and this poses difficulties in measuring cyclotron resonance in metals.

Another restriction on observing cyclotron resonance is that the relaxation time should be long enough for charge carriers to undergo at least $1/2\pi$ of its cyclotron motion:

$$\omega_c \tau = \mu B > 1 \quad (4)$$

As we shall see in the next section, the scattering rate τ^{-1} can be estimated from the absorption peak width and if the scattering rate becomes too large, no distinguishable cyclotron resonance will be observed. The above requirement dictates that the carrier mobility μ should be larger than $10000 \text{ cm}^2/V \cdot \text{s}$ in order to observe cyclotron resonance at a magnetic field strength of 1 T. Hence very pure samples are needed for successful measurement of cyclotron resonance.

The first few experimental demonstrations of cyclotron resonance in determining the carrier effective mass of Si and Ge was carried out in 1950s [1, 2], using microwave radiations.

In both Ge and Si the conduction band edge contains

several spheroids located in equivalent positions in k -space. Close to the band edge, this energy surface is described by:

$$E(\mathbf{k}) = \hbar^2 \left(\frac{k_x^2 + k_y^2}{2m_t} + \frac{k_z^2}{2m_l} \right) \quad (5)$$

where m_l and m_t are the longitudinal and transverse mass parameter, respectively. The magnetic field makes an angle θ with respect to the longitudinal axis of the set of spheroids. For this anisotropic case, the cyclotron mass is no longer the effective mass, but rather components of it [1]:

$$\left(\frac{1}{m^*} \right)^2 = \frac{\cos^2\theta}{m_t^2} + \frac{\sin^2\theta}{m_l m_t} \quad (6)$$

As shown in Fig. 1, the magnetic field makes different angles with the longitudinal axis of the spheroids as it changes from the [001] direction to the [110] direction, leading to different numbers of resonance peaks in the absorption spectra. Each resonance peak leads to an effective mass determined by $m = eB/\omega_c$ and by fitting this angular dependence one can determine the longitudinal and transverse mass parameters, which finally determine the effective mass or equi-energy surface.

Magneto-Optical Faraday Effect, first discovered by Michael Faraday in 1845, describes the phenomena that linearly polarized light transmitted through the sample experiences changes in polarization angle and ellipticity when a magnetic field or magnetization is present. Faraday Effect is the first observation of light-magnetism interaction. Faraday rotation, along with Kerr rotation which describes the change of polarization angle and ellipticity of the reflected light, has been widely studied in semiconductors, high temperature superconductors, topological insulators and graphene both experimentally [4, 6–8] and theoretically [9, 10].

Faraday rotation measurement can be thought of an "optical analogue" of DC Hall effect and extends the sensitivity to type of charge carriers to a broader energy range.

II. DEVELOPMENT

Following the first experiment in the 1950s on cyclotron resonance (CR), many have tended to the problem of measuring CR in metals. A special geometry called **Azbel-Kaner** geometry [5] is used where the magnetic field is now parallel to the sample surface. The oscillating electric field is also parallel to the sample surface while perpendicular to the magnetic field. Electron undergoes Larmor motion along the field line, and moves in and out of the skin depth region periodically. When the oscillating

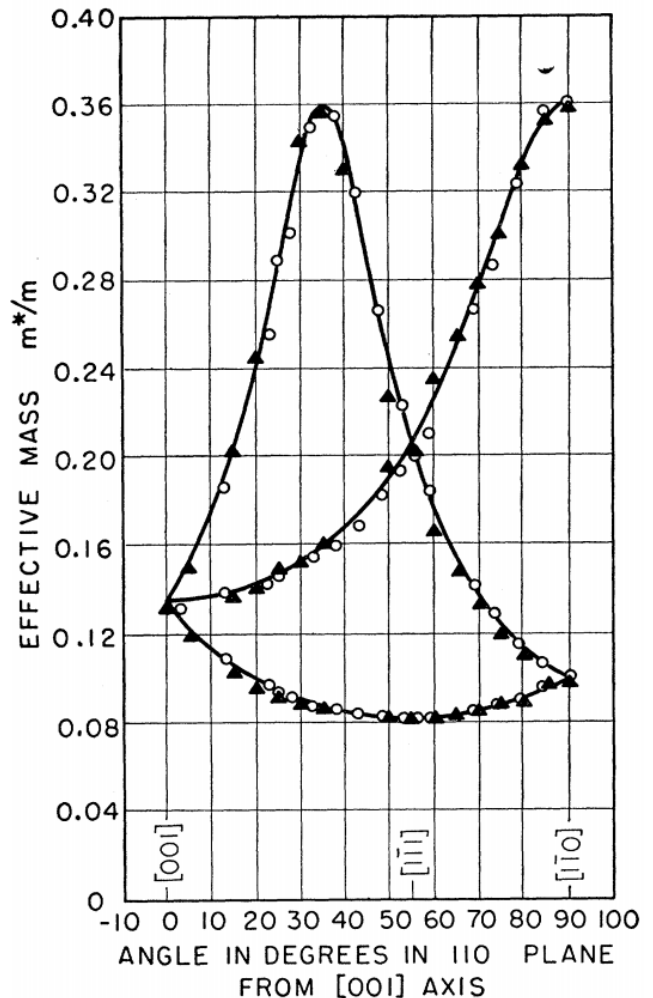


FIG. 1. Effective mass for Ge at 4 K normalized by electron mass. The magnetic field direction is in the (110) plane. Solid curves are fit calculated using Eq. 6, with $m_l = 1.58m$, $m_t = 0.082m$ [1]

electric field has frequency that satisfies $\omega = n\omega_c$ then the electron will be accelerated every time it enters the skin depth zone and therefore absorbs energy from the electric field. In the 1960s the Azbel-Kaner geometry was utilized to study the Fermi surface in many metals e.g. Cu, Te, Sb, Bi [11–15]. However, the data analysis can be complicated as to which orbits contribute most to the cyclotron resonance.

Another development is the realization that the condition $\omega_c\tau = \mu B > 1$ can be more easily satisfied in the THz (10^{12} Hz) or far-infrared region. With the corresponding magnetic field lies in the range of a few Tesla and is readily available to many steady-state magnets in labs. Many of the contemporary cyclotron resonance measurements are therefore using Terahertz Time-Domain Spectroscopy (THzTDS) in two dimensional electron gas (2DEG) [16, 17] and n-InSb [18] or Fourier Transform

Infrared Spectroscopy (FTIR) in many compound semiconductors [19–22] and recently in graphene [8].

III. THEORETICAL BACKGROUND

In this section I will derive the theoretical background of cyclotron resonance and Faraday effect using semi-classical Drude formalism, specifically the derivation of dynamical conductivity tensor. In principle one can resort to Boltzmann transport theory and Kubo-Greenwood formalism for more rigorous treatment but in many cases the semi-classical model contains enough physical information. Moreover, the following derivation agree with the result obtained from Boltzmann theory in the extreme degenerate case ($T \rightarrow 0$), justify the successful of semi-classical model [3].

When both electric field and magnetic field exist, the Drude equation of motion becomes:

$$m^* \frac{d\mathbf{v}}{dt} + m^* \frac{\mathbf{v}}{\tau} = -e(\mathbf{E} + \mathbf{v} \times \mathbf{B}) \quad (7)$$

where m^* is the effective mass, τ is the relaxation time and \mathbf{v} is the drift velocity. Using harmonically varying field $\mathbf{E} = E_0 e^{-i\omega t}$, the corresponding drift velocity will have the form $\mathbf{v}(t) = v_0 + v e^{-i\omega t}$

$$\mathbf{v} + \mu^*(\mathbf{B} \times \mathbf{v}) = \mu^* \mathbf{E} \quad (8)$$

where the short notation $\tau^* = \frac{\tau}{1-i\omega\tau}$ and $\mu^* = -\frac{e\tau^*}{m^*}$ denotes the complex relaxation time and complex mobility, respectively.

Using some vector identities:

$$\mathbf{B} \cdot \mathbf{v} = \mu^* \mathbf{B} \cdot \mathbf{E} \quad (9)$$

$$\mathbf{B} \times \mathbf{v} = -\mu^* [\mathbf{B}(\mathbf{B} \cdot \mathbf{v}) - \mathbf{v}B^2] + \mu^* \mathbf{B} \times \mathbf{E} \quad (10)$$

The drift velocity can then be expressed as:

$$\mathbf{v} = \frac{\mu^* \mathbf{E} - \mu^{*2}(\mathbf{B} \times \mathbf{E}) + \mu^{*3} \mathbf{B}(\mathbf{B} \cdot \mathbf{E})}{1 + \mu^{*2} B^2} \quad (11)$$

Current density is related to electric field by the conductivity tensor:

$$\mathbf{J} = -ne\mathbf{v} = \sigma \cdot \mathbf{E} \quad (12)$$

Writing the last equality in the component form, noticing that $\omega_c = \frac{eB}{m^*}$ and using Levi-Civita symbol ε_{ijk} : $\varepsilon_{ijk} = -\varepsilon_{jik}$, the dynamical conductivity can be written as following:

$$\sigma_{ij} = \frac{ne^2\tau^*}{m^*} \cdot \frac{\delta_{ij} - (\omega_c\tau^*)\varepsilon_{ijk}(B_k/B) + (\omega_c\tau^*)^2(B_iB_j/B^2)}{1 + (\omega_c\tau^*)^2} \quad (13)$$

Here the frequency dependence of the conductivity tensor is contained in the complex relaxation time $\tau^* = \frac{\tau}{1-i\omega\tau}$, with the relaxation time τ considered to be a constant.

Next, consider a usual experimental geometry which put magnetic field in z direction (perpendicular to the sample surface) $\mathbf{B} = (0, 0, B)$, the general conductivity

tensor is $\sigma = \begin{pmatrix} \sigma_{xx} & \sigma_{xy} & 0 \\ \sigma_{yx} & \sigma_{yy} & 0 \\ 0 & 0 & \sigma_{zz} \end{pmatrix}$ with elements:

$$\begin{aligned} \sigma_{xx} &= \sigma_{yy} \\ &= \frac{ne^2\tau}{m^*} \cdot \frac{1 - i\omega\tau}{(1 - i\omega\tau)^2 + (\omega_c\tau)^2} \\ &= \frac{ne^2}{m^*} \cdot \frac{\gamma - i\omega}{\omega_c^2 - (\omega + i\gamma)^2} \end{aligned}$$

$$\begin{aligned} \sigma_{xy} &= -\sigma_{yx} \\ &= \frac{ne^2\tau}{m^*} \cdot \frac{-\omega_c\tau}{(1 - i\omega\tau)^2 + (\omega_c\tau)^2} \\ &= \frac{ne^2}{m^*} \cdot \frac{-\omega_c}{\omega_c^2 - (\omega + i\gamma)^2} \end{aligned}$$

$$\sigma_{zz} = \frac{ne^2\tau}{m^*} \cdot \frac{1}{1 - i\omega\tau}$$

The conductivity tensor contains all the information about the charge carrier dynamics. Its tensor properties comes from the anisotropy of the magnetic field.

In cyclotron resonance, one measures the absorption which is directly related to the real part of diagonal conductivity:

$$P = \frac{1}{2} \text{Re}(J_x \cdot E_x^*) = \frac{1}{2} E_0^2 \text{Re}(\sigma_{xx}) \quad (14)$$

The real part of the off-diagonal conductivity is related to Faraday rotation angle. To see this, it is easier to express conductivity in circular basis: $\sigma_{\pm} = \sigma_{xx} \pm i\sigma_{xy}$, with the current density $j_{\pm} = j_{xx} \pm ij_{xy} = \sigma_{\pm} E_{\pm}$.

E_{\pm} represents the right- and left- circularly polarized light and σ_{\pm} can be obtained using the above Drude results:

$$\sigma_{\pm} = \frac{ne^2}{m^*} \frac{i}{\omega \mp \omega_c + i\gamma} \quad (15)$$

Let's consider the case of Faraday rotation due to an two dimensional electron gas (2DEG) between an air-substrate interface [23, 24]. This model is also suited to describe the Faraday rotation in graphene [8].

The complex transmission coefficients can be obtained by solving the Maxwell equations with boundary conditions at the interface, yielding:

$$t_{\pm} = \frac{2n_o}{n_o + n_s + Z_0\sigma_{\pm}} = |t_{\pm}|e^{i\phi_{\pm}} \quad (16)$$

where $Z_0 \approx 377\Omega$ is the vacuum impedance and n_o, n_s are the refractive index of air and substrate, respectively.

The Faraday effect comes from the fact that right- and left- circular polarized light travel at different speed $\frac{c}{n_{+}}$ and $\frac{c}{n_{-}}$ inside the medium and therefore the transmitted components have a phase difference. The Faraday rotation angle can then be expressed as:

$$\theta_F = \frac{1}{2} \arg\left(\frac{t_{-}}{t_{+}}\right) = \frac{1}{2} \arg\left(\frac{n_o + n_s + Z_0\sigma_{-}}{n_o + n_s + Z_0\sigma_{+}}\right) \quad (17)$$

When $n_o + n_s \gg \text{Re}(\sigma_p m)$, as is often the case for weakly absorbing material, the Faraday rotation angle can be simplified by noticing that:

$$\tan(\phi_{\pm}) \approx \phi_{\pm} = Z_0 \frac{\text{Im}(\sigma_{\pm})}{n_s + n_s} \quad (18)$$

so the Faraday rotation angle becomes:

$$\theta_F(\omega) = \frac{Z_0}{n_o + n_s} \sigma_{xy}(\omega)$$

In summary, one can probe the diagonal and off-diagonal components of the dynamic conductivity using cyclotron resonance and Faraday rotation, respectively.

III. EXPERIMENTAL TECHNIQUE

Measurement of cyclotron resonance and Faraday rotation are all based on Fourier Transform Infrared Spectroscopy (FTIR). This technique gives information of absorption or Faraday rotation angle in a relatively broad energy range.

The principle of a Fourier transform spectrometer is based on a Michaelson type interferometer consisting of a fixed mirror, a beam splitter and a moving mirror, as shown in Fig 2. The recombined beam from the beam splitter will then go through the sample and then collected by the detector. When the sample is inside a magnetic field this is the magneto-transmission set-up. When the moving mirror is moving across zero-path-difference positions the recombined beam on the beam splitter will constructively interfere. When the moving mirror moves a distance of $\frac{1}{4}\lambda_0$ then the optical path difference (OPD) is now $\frac{1}{2}\lambda_0$ and the path difference between the fixed and moving mirror are now exactly half the wavelength

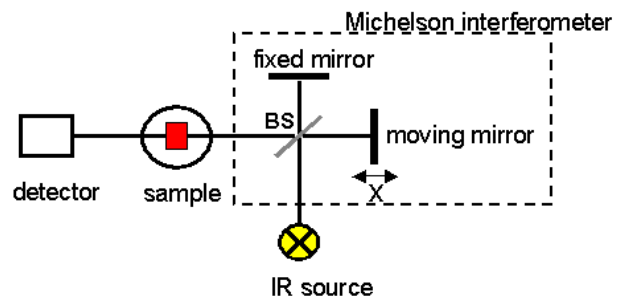


FIG. 2. Schematic of an FTIR

and therefore the beams recombined at the beam splitter will interfere destructively. Another $\frac{1}{4}\lambda_0$ displacement of the moving mirror will again make the recombined beam constructively interfere at the beam splitter. If the moving mirror is moved at constant velocity the signal at the detector will vary sinusoidally. Each time the mirror passes a position where the OPD is multiples of λ_0 there will be a maximum in the detected signal. Thus an interferogram will be generated:

$$S(t) = \int_{-\infty}^{\infty} B(\nu) \cos(2\pi\nu t) d\nu \quad (19)$$

by inverse Fourier transform the interferogram:

$$B(\nu) = \int_{-\infty}^{\infty} S(t) \cos(2\pi\nu t) dt \quad (19)$$

one obtains the spectrum of, in this case, Transmittance.

The sample is inside a split-coil magnet which can provide a magnetic field strength for up to 8 T. The sample is usually cooled with Helium exchange gas and can be maintained as low as 5K, enough for suppress various scattering and achieve longer scattering time.

The detector commonly used in the far infrared range is a He cooled Bolometer and the broadband light source are typically mercury arc lamp (for the very far infrared, 20 cm^{-1} to 100 cm^{-1}) and Globar (for the far infrared 40 cm^{-1} to 1000 cm^{-1})

Two crossed polarizers are used to determine the Faraday rotation angle if the rotation angle is not too small (less than 0.1 degrees). One fixed polarizer (polarizer) is placed before the sample and one rotating polarizer (analyzer) is placed after the sample, usually right in front of the detector. When the field is on, the transmitted light will have a finite Faraday rotation angle (typically a few degrees). By rotating the analyzer over a fixed number of points and measure the intensity of transmitted light one can find the Faraday rotation angle by fitting a $\cos^2(\theta - \theta_F)$ function.

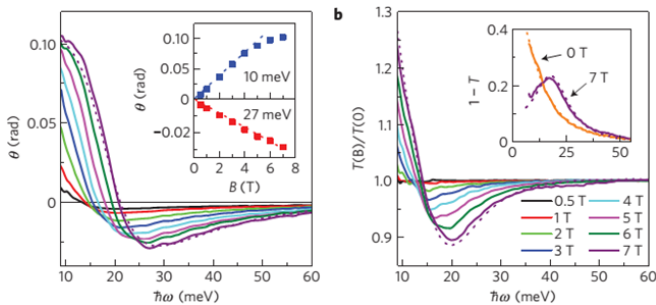


FIG. 3. Faraday rotation and Transmission measurement in single layer graphene grown on SiC substrate [8] corresponding to the blue curve in model Fig. 4

IV. GIANT FARADAY ROTATION IN GRAPHENE

The fact that a single layer of carbon atom gives rise to a Faraday rotation of more than 6 degrees is quite surprising. Considering that in general Faraday rotation angle increase with the thickness of the sample the Faraday rotation of an atomic layer should be within a few milli-radians.

Here I will demonstrate that the giant Faraday rotation is indeed due to the cyclotron resonance.

Fig.3 shows the data of a transmission and Faraday rotation measurement using FTIR. From the right panel, a clear cyclotron resonance absorption is observed and the scattering rate at 7 T can be estimated by the peak width to be around 10 meV. The Faraday rotation is positive at low frequencies and changes sign at higher frequencies, typical of resonance feature.

Follow the formula derived in section II., the Faraday rotation angle can be approximated by the real part of off-diagonal conductivity $Re[\sigma_{xy}]$. So it will be beneficial if we model the behavior of $Re[\sigma_{xy}]$ around cyclotron frequency. The result is shown in Fig 4.

It can be readily seen that the derivative of off-diagonal conductivity $d\sigma_{xy}/d\omega$ is maximized around at cyclotron frequency ω_c and, although the Faraday rotation angle changes sign when going across ω_c , the sign of the derivative $d\sigma_{xy}/d\omega$ matches the sign of ω_c . Since electrons are defined to have positive cyclotron frequency $\omega_c = eB/m^*$ and holes are defined to have negative cyclotron frequency. The negative slope observed in the Faraday rotation data in Fig 3. therefore demonstrate that the sample is hole doping (Fermi energy is in the valence band).

The Faraday rotation and cyclotron resonance in multilayer graphene is very different. First one can identify that since the Faraday rotation around cyclotron frequency has a positive slope, it correspond to electron doping which means that the Fermi energy reside in the conduction band.

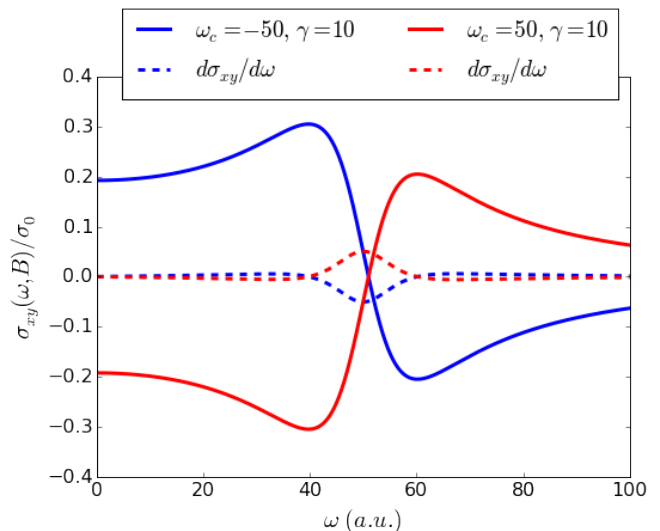


FIG. 4. Model calculation of the off-diagonal conductivity with cyclotron frequency 50 and scattering rate 10. Dashed line is its derivative. Blue and red use opposite value of cyclotron frequency. Note the enhancement of σ_{xy} near ω_c

Secondly, the existence of multiple transitions besides the lower energy cyclotron resonance demonstrate that the different layers are electronically separate and the system is in the so called quantum region. This is resulting from the fact that multilayer graphene are relatively less doped by the SiC substrate compared to the single layer graphene.

For conventional two-dimensional electron gas, electron motions are quantized into a series of equi-spaced Landau-Levels:

$$\mathbf{E}_N = (N + 1/2)\hbar\omega_c \quad (19)$$

This quantization becomes important when the system is in the quantum region $\hbar\omega_c > k_B T$.

The cyclotron resonance can now be viewed as inter-Landau-Level transitions in the quantum description.

Graphene has an unusual linear dispersion relation where the conduction band and valence band touches at the Dirac point. This leads to non-equally spaced Landau-Levels [8]:

$$E_n = \text{sign}(n)\sqrt{2e\hbar v_F^2 |nB|} \quad (19)$$

where $n = 0, \pm 1, \pm 2, \dots$, v_F is the Fermi velocity and B is the perpendicular magnetic field. This \sqrt{B} dependence is observed from the data in Fig. 5 and by fitting this curve one can evaluate the Fermi velocity.

Again, the positive slope at various inflection point of the Landau-Level transition indicates that the transition involves electron-like states.

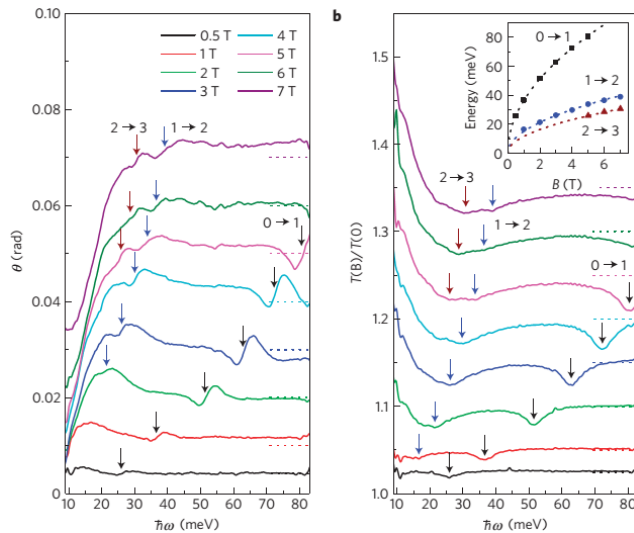


FIG. 5. Faraday rotation and Transmission measurement in multilayer graphene grown on SiC substrate [8] corresponding to red curve in Fig. 4. Inset shows a set of Landau-Level transition is observed and follow the \sqrt{B} dependence

In summary, FTIR based magneto-transmission measurements and Faraday rotation measurements are convenient and contactless methods to measure the diagonal and off-diagonal conductivity. The giant Faraday rotation in graphene comes majorly from the fact that Faraday rotation is enhanced near cyclotron resonance $\omega = \omega_c$. Classical regime cyclotron resonance and quantum regime Landau-Level transitions are observed in single layer graphene and multilayer graphene, respectively. The Faraday rotation measurement allows simultaneously determine the charge carrier type involved in these resonances and transitions.

* y8shao@physics.ucsd.edu

- [1] G. Dresselhaus, A. F. Kip, and C. Kittel, Phys. Rev. 98, 368 (1955).
- [2] B. Lax, H. Zeiger, R. Dexter, and E. Rosenblum, Phys. Rev. 93, 1418 (1954).
- [3] E. D. Palik and J. K. Furdyna, Reports on Progress in Physics 33, 1193 (1970).
- [4] J. Cerne, D. C. Schmadel, L. B. Rigal, and H. D. Drew, Rev. Sci. Inst. 74, 4755 (2003).
- [5] M. Y. Azbel' and E. A. Kaner, Journal of Physics and Chemistry of Solids 6, 113 (1958).
- [6] M. -H. Kim, V. Kurz, J. Opt. Soc. Am. B (2011).
- [7] J. N. Hancock, J. L. M. van Mechelen, A. B. Kuzmenko, D. van der Marel, C. Brüne, E. G. Novik, G. V. Astakhov, H. Buhmann, and L. W. Molenkamp, Phys. Rev. Lett. 107, 136803 (2011).
- [8] I. Crassee, J. Levallois, A. L. Walter, M. Ostler, A. Bostwick, E. Rotenberg, T. Seyller, D. van der Marel, and A. B. Kuzmenko, Nat Phys 7, 48 (2011).
- [9] J. Maciejko, X.-L. Qi, H. D. Drew, and S.-C. Zhang, Phys. Rev. Lett. 105, 166803 (2010).
- [10] W.-K. Tse and A. H. MacDonald, Phys. Rev. B 84, 205327 (2011).
- [11] A. Kip, D. Langenberg, and T. Moore, Phys. Rev. 124, 359 (1961).
- [12] W. Datars and R. Dexter, Phys. Rev. 124, 75 (1961).
- [13] C. Grimes and A. Kip, Phys. Rev. 132, 1991 (1963).
- [14] Y. Couder, Phys. Rev. Lett. 22, 890 (1969).
- [15] Y.-H. Kao, Phys. Rev. 129, 1122 (1963).
- [16] X. Wang, D. J. Hilton, L. Ren, D. M. Mittleman, J. Kono, and J. L. Reno, Opt. Lett. 32, 1845 (2007).
- [17] X. Wang, D. J. Hilton, J. L. Reno, D. M. Mittleman, and J. Kono, Opt. Express 18, 12354 (2010).
- [18] T. Arikawa, X. Wang, A. A. Belyanin, and J. Kono, Optics Express 20, 19484 (2012).
- [19] A. Moll, C. Wetzel, B. K. Meyer, P. Omling, and F. Scholz, Phys. Rev. B 45, 1504 (1992).
- [20] E. D. Palik, S. Teitler, and R. F. Wallis, Journal of Applied Physics 32, 2132 (1961).
- [21] Y. Guldner, J. P. Vieren, P. Voisin, M. Voos, L. L. Chang, and L. Esaki, Phys. Rev. Lett. 45, 1719 (1980).
- [22] M. Suzuki, K. Fujii, T. Ohyama, H. Kobori, and N. Kotera, J. Phys. Soc. Jpn. 72, 3276 (2003).
- [23] R. F. O'Connell and G. Wallace, Phys. Rev. B 26, 2231 (1982).
- [24] K. W. Chiu, T. K. Lee, and J. J. Quinn, Surface Science 58, 182 (1976).